X-641-67-506

NASA TM X-55975

THE AURORAL O_2-DISSOCIATION AND THE INFRARED OH-EMISSION

KAICHI MAEDA

OCTOBER 1967

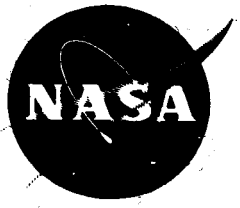

GODDARD SPACE FLIGHT CENTER

GREENBELT, MARYLAND

Presented at the Birkeland Symposium on Aurora and Magnetic Storms, Sandefjord, Norway, September 1967

X-641-67-506

THE AURORAL O_2-DISSOCIATION AND THE INFRARED OH-EMISSION

Kaichi Maeda

October 1967

GODDARD SPACE FLIGHT CENTER
Greenbelt, Maryland

The Auroral O_2-Dissociation and the Infrared OH-Emission

by
Kaichi Maeda
NASA-Goddard Space Flight Center
Greenbelt, Maryland

ABSTRACT

It is shown that the dissociation of molecular oxygen in the polar upper atmosphere caused by auroral particles is accompanied by the increase of ozone in the dissociating layer, contrary to that due to the solar UV-radiation (Maeda, Aikin, 1967). Since hydrogen-ozone reaction is one of the most effective sources for the atmospheric hydroxyl emission (OH vibrational-rotation band airglow), one would expect an enhancement of the OH-emission, following auroral O_2-dissociation. Present calculations based on the time dependent chemical equations for the hydrogen-oxygen atmosphere indicates, however, that the intensity of OH-infrared emission does not enhance during usual quiet auroras, except in the lower borders of the so-called (purplish-red) Type B auroras. The extension of the Monte Carlo calculation of the electron-diffusion in the upper atmosphere (Maeda, 1965) to the case of the atmosphere with constant vertical magnetic field is also presented, indicating a drastic confining effect of the magnetic field on the horizontal spread of the impinging electron flux.

(1) Maeda, K. and A. C. Aikin; Temporal Variations of Mesospheric Oxygen and Ozone During Auroral Events, NASA Tech. Note D-3993, (1967)

(2) Maeda, K.; Diffusion of low energy auroral electrons in the atmosphere, J. Atmos. Terr. Phys. 27, 259-275, (1965)

1. Introduction

The rate of dissociation of molecular oxygen by auroral electrons and consequent variations in the temporal and the vertical distributions of the oxygen allotropes were calculated with respect to the isothermal, pure-oxygen atmosphere (Maeda and Aikin, 1967 a, b*).

In this paper, similar calculations are made with respect to the non-isothermal, hydrogen-oxygen atmosphere to see the subsequent auroral effects on the hydroxyl emission.

The previously reported Monte-Carlo calculation of electron diffusion in the upper atmosphere (Maeda, 1965 a, b) is also extended to the atmosphere with a constant vertical magnetic field. Although this new result of the diffusion of auroral electrons in the polar atmosphere does not alter the previous conclusions (MA-I and II), the effect of the geomagnetic field on the horizontal spreads of impinging electron beams is remarkable. Since these are not essential for the present problem, the details of the computations on the electron diffusion in the atmosphere with the geomagnetic field will be presented elsewhere (Berger, Maeda and Seltzer, 1968).

2. Auroral Dissociation of the Atmospheric Oxygen

2.1 Dissociation of Oxygen Molecules by Electron Impacts.

Due to the great improvements in the energy-resolution and control of mono-energetic electron beam in the laboratory experiments, the cross-sections of molecular dissociations as well as excitations and of ionizations have recently been measured very accurately, almost comparable to those of optical experiments.

The oxygen molecule has the large electron-impact cross-section for dissociation with a maximum around 8.4 eV, corresponding to the photodissociation due to the Schumann-Runge UV radiations (1400 $\sim$ 2000 Å).

These cross-sections are shown in Figure 1 as a function of the energy of colliding electrons. In the figure, the meanings of each

---

*These will be referred to as MA-I and MA-II, respectively.

cross-section are as follows; (i) σ^-, the dissociative attachment of an electron i.e.

$$O_2 + e \longrightarrow O + O^- \qquad (2.1)$$

This has a peak (1.6×10^{-18} cm^2) at 6.5 eV (Rapp et al., 1964 a, b). (ii) σ_i, the total ionization, including dissociative ionization such as

$$\begin{aligned} O_2 + e &\longrightarrow O + O^+ + 2e \\ &\quad O^- + O^+ + e \\ &\quad O^+ + O^+ + 3e \quad \text{etc.} \end{aligned} \qquad (2.2)$$

With increasing energy of electron, the multiple ionization (O^{++}, O^{+++}) appears in the secondary products (Frost and McDowell, 1958). In this figure, σ_i is taken from the result given by Tates and Smith (1932). (iii) σ_{SL} ; molecular dissociation into two neutral atoms, i.e.

$$O_2 + e \longrightarrow O + O^* + e \qquad (2.3)$$

where O and O* are mostly ^{3}P and ^{1}D-states, respectively. It should be noted that this cross section is the sum of several cross-sections corresponding to the various transitions between the initial states of oxygen molecules (not only ground state $X\,^3\Sigma_g^-$ but also $a\,^1\Delta_g$ and $b\,^1\Sigma_g^+$) and the final dissociative states (such as $B\,^3\Sigma_u^- \longrightarrow O(^3P) + O(^1D)$, $^1\Delta_u \longrightarrow O(^1D) + O(^1D)$ and $^1\Sigma_u^+ \longrightarrow O(^1D) + O(^1S)$ etc.).

According to Lassettre et al. (1964), and Silverman et al. (1964), the maximum cross-section for the electron impact O_2-dissociation is of the order of 4×10^{-16} cm^2 above 8.4 eV. It should also be noted that above approximately 18.7 eV dissociation is accompanied by ionization as shown in (2.2).

σ_{BB} is the cross-section corresponding to (2.3) calculated by Bauer and Bartky (1965) based on the classical theory of Gryzinski (1959), which gives a lower bound on the electron impact dissociation

cross section, since only one transition has been taken into account. σ_M is the similar cross section used by Maeda (1962, 1963) which was derived by combining the measurements of Glockler and Wilson (1932) below 20 eV and theoretical extrapolation above 100 eV (Massey and Burhop, 1956). Figure 1 indicates that the rate of O_2-dissociation by electron impacts based on σ_M was nearly two order of magnitude underestimated as compared to the latest laboratory data.

Finally, the recent semi-empirical expression of electron impact cross-sections for molecular oxygen given by Green and Dutta (1967) and Watson et al. (1967) agrees with σ_i shown in Figure 1. Their cross section for excitations into the Schumann-Runge band and continuum seems, however, to be too small, if not neglected, even compared to theoretical results of Bauer and Bartkey (1965).

2.2 Diffusion of Auroral Electrons in the Polar Atmosphere.

Due to the fluctuations in energy loss (straggling) and multiple scattering, the energy distribution of penetrating electrons in the atmosphere becomes broader with increasing depth of penetration even if the initial primary electrons are monoenergetic.

This is shown in Figure 2 where $i(E_0, E, \xi)$; the number of electrons with energies between E and E + dE at the depth ξ, corresponding to the incident energy E_0, is plotted against E with the parameter ξ. Non-dimensional penetration depth ξ is defined by the ratio of the actual penetration depth in the atmosphere (in g/cm^2) to an empirical range r_0 (in g/cm^2) which is given by

$$r_0 = c E_0^{7/4} \tag{2.4}$$

where E_0 is the initial energy in kev and $c = 4.57 \times 10^{-6}$ (Grün, 1957). It should be noted that these calculations are possible only by means of the Monte-Carlo method (Berger, 1963).

For the practical applications, the results of Monte-Carlo calculations are approximated by the empirical formula (MA-I, II). These are also shown in Figure 2 by dashed lines. As already mentioned, in these calculations of electron diffusion in air, the energy losses by atomic collisions, multiple coulomb scattering as well as straggling (statistical fluctuations in energy loss) are simultaneously taken into

account, but the effect of the earth's magnetic field is, however, completely neglected. It was shown, however, that as long as the energy dissipations in each horizontal layers are concerned, the vertical magnetic field parallel to the incident direction has no effect on the results (MA-I, II). The effect of the vertical magnetic field is simply to reduce the horizontal spread of electron beam by curving the orbits of each free electrons between their collisions in air. This effect is, however, very remarkable as shown in Figure 3 where the mean horizontal radius, R_0, of vertically incident electron beam with initial energy E_0 = 50 kev is plotted against altitude z (in km), for three cases of vertical magnetic field H i.e. H = 0, 0.3 and 0.6 gauss. The definition of mean horizontal radius R_0 and some other related quantities are discussed in Appendix A.

From this figure, one can see that the horizontal spread of auroral electron beams are confined by the vertical earth's magnetic field of 0.6 gauss within the range of less than 100 m, which should extend upto nearly 10 km, if there is no geomagnetic field.

In Figure 4, the gyroradius R_c (in meter) of 50 kev electron in the 0.6 gauss field and the gas-kinematic mean free path R_f (in meter) for 50 kev electron are shown for comparison, indicating the importance of magnetic control of horizontal spread even below the altitude of 100 km, where collisions dominate i.e. the collision frequency between electron and air molecules and ions, ν_e, exceeds the gyrofrequency of electron in 0.6 gauss, ω_c (Chapman, 1956).

Finally, the horizontal spread of auroral electrons and their vertical distributions are shown in Figure 5 for incident energies, E_0 = 400/n kev, where n = 1, 2 · · · 8. The results for $E_0 \lesssim 4$ kev are, however, not conclusive because of inaccuracies in energy loss near the terminating point of electron path i.e. the relative accuracy decreases near the cut-off energy computation (Berger, Maeda and Seltzer, 1968).

2.3 Rate Coefficient for Auroral O_2-Dissociation

The rate of dissociation of atmospheric oxygen molecules by the monoenergetic primary electron, E_0, at the altitude z can be given by

$$J_{de}(z, E_0) = \int_0^{E_0} N(z) \left[\int_{E_c}^{E} \sigma_d(w)\, j_e(w, E, z)\, dw \right] i(E_0, E, z)\, dE\, dz \quad (2.5)$$

where

N(z) is the number density of molecular oxygen at the altitude z, (cm^{-3}).

$\sigma_d(w)$ is the differential cross-section of O_2-dissociation by electrons with energy w (cm^2, w is kev).

$j_e(w, E, z)$ is the number of secondary and tertiary electrons of energy between w and w + dw, produced by electrons of energy E per unit thickness of air at the altitude z(cm^{-1}, z in km).

$i(E_0, E, z)$ is the number of electrons with energies between E and E + dE at the altitude z, corresponding to the incident energy E_0.

E_c is the threshold energy for O_2-dissociation and assumed to be 5 eV.

As mentioned in Appendix A, transformation from $i(E_0, E, \xi)$ to $i(E_0, E, z)$ is made with respect to the CIRA (1964) atmosphere. The actual calculations of $J_{de}(E_0, z)$ are performed numerically, using σ_{SL} shown in Figure 1 as $\sigma_d(w)$ with several approximations (MA-I and II). The results are shown in Figure 6.

According to the direct measurements by rockets (McIlwain, 1960; Evans, 1966) and by satellites (O'Brien, 1964), the energy spectrum as well as intensities of auroral electrons fluctuate widely within the order of hundred meters and within a fraction of a second. If one takes the spatial and temporal average over the range of several hundred meters and several minutes, the incident auroral electron spectra are expressed with a good approximation by

$$i(E_0) = i_0 \exp\left(-\frac{E_0}{E_a}\right) \qquad (2.6)$$

where E_a is a constant and around 10 kev or less in most cases of bright aurora. E_a is reported occasionally as high as 100 kev during the events of auroral absorption (Brown, 1964, 1966; Bailey et al., 1966). The rate of O_2-dissociation by the auroral electrons with these energy spectra are calculated as follows: using the previous results for monoenergetic electrons;

$$J_D(z, E_a) = \frac{\int_0^\infty J_{ae}(z, E_0)\, c^{-E_0/E_a}\, dE_0}{\int_0^\infty \exp\left(-\frac{E_0}{E_a}\right) dE_0}$$

$$\simeq \frac{1}{E_a} \sum_{i=1}^{\infty} J_{de}(z, E_0^i) \exp\left(-\frac{E_0^i}{E_a}\right) \Delta E_0^i \qquad (2.7)$$

where $J_{de}(z, E_0^i)$'s are given by (2.5) and shown in Figure 6.

Considering two rather extreme cases of soft and hard spectrum of auroral electrons, $J_D(z, E_a)$'s are calculated for E_a = 5 kev (soft spectrum) and 100 kev (hard spectrum) as shown in Figure 7.

3. Variations of Oxygens and Hydroxyl During Auroral Events

3.1 Equations and Constants for Chemical Reations.

All reactions in hydrogen-oxygen atmosphere are discussed by Hesstvedt (1964). The principal reactions considered in the present calculation are shown in Table 1. In this table, $J_1, J_2 \cdots J_4$ and $k_1, k_2 \cdots k_{20}$ are the rate coefficients for dissociations and each chemical reactions. The numerical values of these coefficients and their temperature dependences are shown in Table 2. Some of these coefficients are not known accurately as others such as k_1, k_2 and J_2.

3.2 The First Approximations (Constant Nighttime Atomic Hydrogen).

Since the main purpose of the present paper is to see the effect of auroral electrons on the hydroxyl night sky emission, the following three equations are used in the preliminary analysis. This approximation was used by several investigators for the nighttime (after sun-set) enhancement of hydroxyl emission (Wallace, 1962; Ballif and Venkateswaran, 1963)

$$\frac{d[O]}{dt} = 2J_2[O_2] + J_3[O_3] - 2k_1[M][O]^2 - k_2[O][O_2][M] - k_3[O][O_3] - k_6[O][OH] - k_8[O][HO_2] \qquad (3.1)$$

$$\frac{d[O_3]}{dt} = k_2[O][O_2][M] - k_3[O][O_3] - k_4[H][O_3] - J_3[O_3] \qquad (3.2)$$

$$\frac{d[H]}{dt} = J_1 [H_2O] + k_6 [OH] [O] - k_4 [H] [O_3] - k_9 [H] [O_2] [M] \qquad (3.3)$$

$$[O] + 2[O_2] + 3[O_3] = f(z) \qquad (3.4)$$

where $J = J_\lambda + J_e$ and f(z) is a function of altitude. During the night time, photo-dissociation is zero (i.e. $J_\lambda = 0$) and variations of hydrogen atom can be neglected (Wallace, 1962) then from Equation (3.3), we get

$$[OH] = [H]\left(k_4 [O_3] + k_9 [O_2] [M]\right)/k_6 [O] \qquad (3.5)$$

Since it is shown that the soft spectrum auroral electrons cause no significant effects on the oxygen allotropes concentrations in the upper atmosphere (MA-I, II), only the hard spectrum case i.e. $E_a = 100$ kev in Equation (2.6) is considered in this paper.

The ineffectiveness of soft auroral electrons on the atmospheric oxygen allotrope variation is due to the very large time constant (i.e. the life time) of atomic oxygen above 90 km level, where most of the oxygen molecules are dissociated by the solar UV-radiation. The decay time τ_1 (in sec.) of the mesospheric oxygen atom is shown in Figure 8, together with that of ozone τ_3 (in sec.). It should be noted that the life time of atmospheric ozone decreases slowly with altitude, while that of atomic oxygen increases drastically above 90 km. The similar curves given by Hunt (1965) are also shown in Figure 8 for a comparison.

Temporal variations of the vertical distribution of the oxygen atom and of ozone caused by the hard spectrum auroral electrons are shown in Figure 9, where the flux of the primary auroral electron is assumed to be 10^{10} electrons per cm^2 sec. The corresponding time variations of hydroxyl concentration calculated under the constant nighttime concentration of atomic hydrogen are shown by dashed lines in Figure 11. As shown by Hunt (1966), the daytime concentration of atomic hydrogen increases below around 85 km, which is indicated by the dashed line in Figure 9.

The result which is based on the time independent nighttime distribution of atomic hydrogen shows that the hydroxyl concentration does not inhance but rather diminishes during hard spectrum auroral events.

The OH-emission corresponding to the initial condition (t = 0 min) indicated by the dashed line in Figure 11, is of the order of 2000 R, provided that the F-factor* is assumed to be 4 (Chamberlain and Smith, 1959).

3.3 The Second Approximation (Time Dependent Nighttime Hydrogen).

Considering all chemical reactions listed in Table 1, we get eight simultaneous time dependent differential equations for the chemical variations at each levels in the atmosphere as shown in Appendix B. Two differential equations are, however, replaced by the additional two conditions which indicate the conservations of oxygens and hydrogens at each level, respectively. These are also shown in Appendix B. Actual calculations to see the auroral effects are made after finishing the marching integration for a period of five days. In other words, the deviations due to the arbitrary initial conditions (i.e. HO_2, HO, O and O_3 an be assumed to be zero at the beginning, for example) are eliminated by computing the diurnal variations of these compounds, including the photodissociations by the solar UV-radiations.

The variations of the concentrations of atomic oxygen $[O]$, ozone $[O_3]$ and atomic hydrogen $[H]$ due to the auroral electrons with flux 10^{10} electrons per cm^2 per second are shown in Figure 10, and the corresponding variation of OH is shown in Figure 11 by full lines.

4. Conclusions

The vibration-rotation bands of hydroxyl (OH) discovered by Meinel (1950) is one of the brightest airglow in night sky. The enhancement of this emission after the sunset, which sometimes exceeds 5000 kR, is well-explained by hydrogen-ozone reactions (2.4) in Table 1 proposed by Bates-Nicolet (1950). As shown by Wallace (1962), so far the following observational features have been known:

(1) The total intensity of emission at its maximum which occurs around hours after the sunset is of the order of 5000 kR or more.

(2) The height of emission is between 75 km and 90 km with a maximum around 85 km.

*Average number of photons emitted per excited OH-molecule (cf. Hunt, 1966).

(3) The emission ranges from hardly visible 5000 Å region to far infrared 4.5μ with maximum around 2.3 ~ 3.6μ .

(4) The emission band intensity drops sharply beyond v = 9, indicating that the excitation of atmosphere hydroxyl is up to 3.3 eV.

(5) Generally, the emission is stronger in winter than in summer, although day-to-day fluctuation is occasionally very large.

(6) Relations of OH-emission intensity and its fluctuation to the geomagnetic activity and solar activities are not well-established.

Considering the above feature, especially the nighttime enhancement due to hydrogen ozone reaction, one would expect the enhancement of OH-emission during hard spectrum auroras.

The present calculation shows, however, that hydroxyl emission does not enhance but rather decreases, if the nighttime concentration of hydrogen atom is assumed to be constant as shown by dashed lines in Figure 11. This indicates a fundamental difference between the photo-dissociations of the atmospheric oxygens due to the solar UV-radiation and the auroral dissociations. This difference can be attributed to the steep decrease of the solar UV-intensity in the shorter wavelength. Namely, the intensity of O_2-dissociating UV-radiation, i.e., Schumann-Runge band and continuum (1400 ~ 2000 Å) is nearly 10^{-4} times of O_3-dissociating radiation, (i.e., Hartley band, 2200 ~ 3000 Å and some visible radiations in Chappins band 4500 ~ 7500 Å).*

In the case of the photo-dissociation by the solar UV-radiation, the increase of atomic oxygen is therefore always accompanied by the decrease of ozone, since the photo-dissociation of ozone (the last term in the right side of Eq. (3.2)) dominates over the production by three body collision (the first term in the right side of Eq. (3.2)).

*The solar spectral irradiances are roughly 10^2 (ergs/cm^2 sec μ) at 1500Å, 3.10^5 (ergs/cm^2 sec μ) at 3000Å and 2.10^6 (ergs/cm^2 sec μ) at 5000Å, respectively.

On the other hand, in the case of auroral dissociation, even the cross-section of ozone is assumed to be more than one hundred times that of molecular oxygen; O_3-dissociation does not dominate over the production by three body collisions below around 80 km. Consequently, an increase of atomic oxygen caused by O_2-dissociation is associated with increase of ozone.

As can be seen from Equation (3.5), the time variation of hydroxyl concentration is essentially proportional to the ratio of atmospheric ozone concentration to oxygen atoms concentration if the variation of hydrogen atom is ignored. Consequently, the concentration of hydroxyl does not increase during auroral events, but rather decreases.

On the other hand, all possible chemical reactions between oxygens and hydrogens are considered, the concentration of atomic hydrogen below 80 km level increases during the auroral events as shown in Figure 10, even though the direct dissociations of water vapor by auroral electrons are neglected. Correspondingly, the concentration of OH increases as shown by full lines in Figure 11. The altitude of the maximum OH-concentration is, however, lower and its vertical distribution is broader than the observed concentrations of OH-emission (Packer, 1961). These results indicate that the auroral enhancement of OH-emission should decay faster than the usual (quiet time) nighttime OH-emissions. Although it is not shown in the present figures, the enhancement of OH-emission based on the second order approximation continues several minutes after the cessation of electron precipitations and decays quickly in the lower atmosphere. The maximum OH-emission expected from the present results (the second order approximation) is only around 400 R (with F-factor 4). If the direct auroral H_2O-dissociation is taken into account, the maximum enhancement of OH-emission should exceed far beyond this value. In the case of strong auroral glow with very large flux of high energy protons, another additional enhancement of OH-emission can be expected together with well-known hydrogen emissions. It should be noted that if the flux of auroral electrons is less than 10^5 per cm^2 sec, no auroral effect can be observed. This can be explained by the domination of loss term over production term in the time dependent chemical equations for atomic oxygen and for ozone.

In the present calculation, the vertical temperature distribution which affects on the rate coefficients as shown in Table 2, is taken from CIRA (1964) atmospheric model. Although it is not expressed explicitly in the present calculations, the photodissociation of water vapor and methane are regarded as the sources of hydrogen atoms in

the upper mesosphere (Nicolet, 1965). It should be noted that in the altitude range where the variations of all oxygen allotropes and hydrogen-oxygen compounds take place, i.e. above 50 km up to 90 km, the dynamical effects of atmospheric motion especially diffusions due to turbulence cannot be neglected. In this respect, the present calculations need further improvement, including the auroral dissociations of water vapor and contributions from auroral protons.

As a summary, the present calculations (the second order approximation) indicate that the hydroxyl infrared emission will be enhanced during strong Type B auroras (the so-called purplish-red lower border), due to the auroral dissociation of atmospheric oxygen molecules and subsequent increase of ozone and atomic hydrogen reaction in the upper mesosphere.

Table 1
Principal Reactions in Hydrogen Oxygen Atmosphere

(1) Dissociations by Photo-Absorption (J_λ) and by Electron-Impact (J_e)

$$H_2O + h\nu,\ (e) \xrightarrow{J_1} OH + H + (e) \quad \text{for } \lambda \leq 2000\text{Å} \text{ and } E \geq 6 \text{ eV} \qquad (1.1)$$

$$O_2 + h\nu,\ (e) \xrightarrow{J_2} O + O + (e) \quad \text{for } \lambda \leq 2400\text{Å} \text{ and } E \geq 5 \text{ eV} \qquad (1.2)$$

$$O_3 + h\nu,\ (e) \xrightarrow{J_3} O_2 + O + (e) \quad \text{for } \lambda \leq 11800\text{Å} \text{ and } E > 1 \text{ eV} \qquad (1.3)$$

$$HO_2 + h\nu,\ (e) \xrightarrow{J_4} OH + O + (e) \quad \text{for } \lambda \lesssim 12000\text{Å} \text{ and } E \gtrsim 1 \text{ eV} \qquad (1.4)$$

where $J_i = J_{i\lambda} + J_{ie}$

Table 1 (Continued)

(2) Chemical Reactions by Collision

$$O + O + M \xrightarrow{k_1} O_2 + M \quad (2.1)$$

$$O + O_2 + M \xrightarrow{k_2} O_3 + M \quad (2.2)$$

$$O + O_3 \xrightarrow{k_3} O_2 + O_2 \quad (2.3)$$

$$H + O_3 \xrightarrow{k_4} OH + O_2 \quad (2.4)$$

$$H + O_3 \xrightarrow{k_5} HO_2 + O \quad (2.5)$$

$$OH + O \underset{k_7}{\overset{k_6}{\rightleftharpoons}} H + O_2 \quad (2.6)\ (2.7)$$

$$HO_2 + O \xrightarrow{k_8} OH + O_2 \quad (2.8)$$

$$H + O_2 + M \xrightarrow{k_9} HO_2 + M \quad (2.9)$$

$$H + O + M \xrightarrow{k_{10}} OH + M \quad (2.10)$$

$$H + HO_2 \xrightarrow{k_{11}} H_2O + O \quad (2.11)$$

$$H + HO_2 \xrightarrow{k_{12}} H_2 + O_2 \quad (2.12)$$

$$H + HO_2 \xrightarrow{k_{13}} OH + OH \quad (2.13)$$

$$H + H + M \xrightarrow{k_{14}} H_2 + M \quad (2.14)$$

$$H + OH \underset{k_{16}}{\overset{k_{15}}{\rightleftharpoons}} H_2 + O \quad (2.15)\ (2.16)$$

$$H_2 + OH \xrightarrow{k_{17}} H_2O + H \quad (2.17)$$

$$OH + O_3 \xrightarrow{k_{18}} HO_2 + O \quad (2.18)$$

$$OH + OH \xrightarrow{k_{19}} H_2O + O \quad (2.19)$$

$$OH + HO_2 \xrightarrow{k_{20}} H_2O + O_2 \quad (2.20)$$

Table 2
Numerical Values of Chemical Rate Coefficients
Corresponding to the Reactions Shown in Table 1

$k_1 = 5 \times 10^{-34} \sqrt{T}$ ($cm^6\ sec^{-1}$) (Nicolet-Bates, 1950)

$k_2 = 8 \times 10^{-35} \exp\left(\frac{445}{T}\right)$ ($cm^6\ sec^{-1}$) (Benson-Axworthy, 1965)

$k_3 = 5.6 \times 10^{-11} \exp\left(-\frac{2850}{T}\right)$ ($cm^3\ sec^{-1}$) (Benson-Axworthy, 1965)

$k_4 = 1.5 \times 10^{-11} \sqrt{T} \exp\left(-\frac{1500}{T}\right)$ ($cm^3\ sec^{-1}$) (Wallace, 1962)

$k_5 = 1.5 \times 10^{-11} \sqrt{T} \exp\left(-\frac{2000}{T}\right)$ ($cm^3\ sec^{-1}$) (Wallace, 1962)

$k_6 = 6.7 \times 10^{-12} \sqrt{T} \exp\left(-\frac{250}{T}\right)$ ($cm^3\ sec^{-1}$) (Hesstvedt, 1964)

$k_7 = 3.6 \times 10^{-9} \sqrt{T} \exp\left(-\frac{12,000}{T}\right)$ ($cm^3\ sec^{-1}$) (Hesstvedt, 1964)

$k_8 = 6 \times 10^{-13} \sqrt{T}$ ($cm^3\ sec^{-1}$) (Hesstvedt, 1964)

$k_9 = 6 \times 10^{-37} \sqrt{T}$ ($cm^6\ sec^{-1}$) (Hesstvedt, 1964)

$k_{10} = 6 \times 10^{-34} \sqrt{T}$ ($cm^6\ sec^{-1}$) (Wallace, 1962)

$k_{11} = 1.5 \times 10^{-11} \sqrt{T} \exp\left(-\frac{2000}{T}\right)$ ($cm^3\ sec^{-1}$) (Hesstvedt, 1964)

$k_{12} = 2 \times 10^{-13} \sqrt{T}$ ($cm^3\ sec^{-1}$) (Hesstvedt, 1964)

$k_{13} = 6 \times 10^{-13} \sqrt{T}$ ($cm^3\ sec^{-1}$) (Hesstvedt, 1964)

$k_{14} = 1.6 \times 10^{-33} \sqrt{T}$ ($cm^6\ sec^{-1}$) (Hesstvedt, 1964)

$k_{15} = k_5 = 1.5 \times 10^{-11} \sqrt{T} \exp\left(-\frac{2000}{T}\right)$ ($cm^3\ sec^{-1}$) (Wallace, 1962)

Table 2 (Continued)

$k_{16} = 4.5 \times 10^{-11} \sqrt{T} \exp\left(-\frac{3500}{T}\right)$ ($cm^3\ sec^{-1}$) (Wallace, 1962)

$k_{17} = 7 \times 10^{-12} \sqrt{T} \exp\left(-\frac{5000}{T}\right)$ ($cm^3\ sec^{-1}$) (Hesstvedt, 1964)

$k_{18} = 1.5 \times 10^{-11} \sqrt{T} \exp\left(-\frac{2000}{T}\right)$ ($cm^3\ sec^{-1}$) (Hesstvedt, 1964)

$k_{19} = 1.6 \times 10^{-13} \sqrt{T}$ ($cm^3\ sec^{-1}$) (Hesstvedt, 1964)

$k_{20} = k_{13} = 1.6 \times 10^{-33} \sqrt{T}$ ($cm^3\ sec^{-1}$) (Hesstvedt, 1964)

REFERENCES

1. Bailey, D. K., M. A. Pomerantz, K. W. Sullivan, and C. C. Taib, "Characteristics of precipitated electrons inferred from ionosphere forward scatter," J. Geophys. Res. 71, 5179-5182, 1966.

2. Ballif, J. R. and S. V. Venkateswaran, "On the Temporal Variations of the OH-Nightglow," J. Atmos. Sci., 20, 1-4, 1963.

3. Bates, D. R. and M. Nicolet, "The Photochemistry of atmospheric water vapor," J. Geophys. Res. 55, 301-327, 1950.

4. Bauer, E., and C. E. Bartky, "Calculation of inelastic electron-atom and electron molecules collision cross sections by classical methods," Aeronutronic Publication No. U-2943, Philco Corp. 1965.

5. Benson, S. W. and A. E. Axworthy, "Reconsideration of the rate constants from the thermal decomposition of ozone," J. Chem. Phys. 42, 2614-2615, 1965.

6. Berger, M. J., "Monte Carlo Calculation of the Penetration and Diffusion of Fast Charged Particles," published in "Methods in Computational Physics, Vol. 1," Academic Press, Inc. N.Y. 1963.

7. Berger, J. M., K. Maeda and S. Seltzer, "Diffusion of electron in the atmosphere with a constant magnetic field," to be published in J. Atmos. Terr. Phys.

8. Brown, R. R., "Feature of the auroral electron energy spectrum inferred from observations of ionosphere absorption." Arkiv. Geophys. 4, 405-426, 1964.

9. Brown, R. R., "Electron precipitation in the auroral zone," Space Sci. Rev. 5, 311-387, 1966.

10. Chamberlain, J. W. and C. A. Smith, "On the excitation rates and intensities of OH in the airglow," J. Geophys. Res. 64, 611-614, 1959.

11. Chapman, S. "The electrical conductivity of the ionosphere; a Review," Nuovo Cimento, 4, 1385-1412, 1956.

12. Evans, D. S., "Rocket observations of low energy auroral electrons," Goddard Space Flight Center X-611-66-376, 1966.

13. Frost, D. C. and C. A. McDowell, "The ionization and dissociation of oxygen by electron impact," J. Am. Chem. Soc. 80, 6183-6187, 1958.

14. Glockler, G. and J. L. Wilson," the activation of molecular oxygen by electron impact" J. Am. Chem. Soc. 54, 4544-4558, 1932.

15. Green, A. E. S. and S. K. Dutta, "Semi-empirical cross sections for electron impacts," J. Geophys. Res. 72 (5), 3933-3941, 1967.

16. Gryzinski, M., "Classical theory of electronic and ionic inelastic collisions," Phys. Res. 115, 374-383, 1959.

17. Grün, A. E., "Lumineszenz-photometrische Messungen der Energieabsorption im Strahlungsfeld von Elektronenquellen Eindimensionaler Fall in Luft," Zeit. f. Naturf. 12A, 89-95, 1957.

18. Hesstvedt, E., "On the water vapor content in the high atmosphere," Geofys. Publikasjoner, Norvegica 25 (3) 1-18, 1964.

19. Hunt, B. G., "A Non-equilibrium investigation into the diurnal photo-chemical atomic oxygen and ozone variations in the mesosphere," J. Atmos. Terr. Phys. 27, 133-144, 1965.

20. Hunt, B. G., "Photochemistry of ozone in a moist atmosphere," J. Geophys. Res. 71, 1385-1398, 1966.

21. Lassettre, E. N., S. M. Silverman and M. E. Kransnow, "Electron collision cross sections and oscillator strengths for oxygen in the Schumann-Runge region," J. Chem. Phys. 40, 1261-1265, 1964.

22. Maeda, K., "On the heating of the polar upper atmosphere," NASA Tech. Rept. R-141, 1962.

23. Maeda, K., "Auroral dissociation of molecular oxygen in the polar mesosphere," J. Geophys. Res. 68, 185-197, 1963.

24. Maeda, K., "Diffusion of auroral electrons in the atmosphere," NASA Tech. Note D-2612, 1965, a.

25. Maeda, K., "Diffusion of low energy auroral electrons in the atmosphere," J. Atmos. Terr. Phys. 27, 259-275, 1965, b.

26. Maeda, K. and A. C. Aikin, "Temporal Variations of Mesospherics Oxygen and Ozone during Auroral Events," NASA Tech. Note D-3993, 1967 a (MA-I).

27. Maeda, K. and A. C. Aikin, "Variations of Polar Mesospheric Oxygen and Ozone During Auroral Events," Planet. Space Sci. 1967 b (in Press). (MA-II).

28. Massey, H. S. W. and E. H. S. Burhop, "Electronic and ionic impact phenomena," Oxford Press, 1956 (see p. 257).

29. McIlwain, C. E., "Direct measurements of particles producing visual auroras," J. Geophys. Res. 65, 2727-2747, 1960.

30. Meinel, A. B., "OH emission bands in the spectrum of the night sky," Astrophys. J. 112, 120-130, 1950.

31. Nicolet, M., "Le problème physique de la stratosphère à la thermophère inférieure," Proc. Roy. Soc. 288 (1415), 478-589, 1965.

32. O'Brien, B. J., "High-latitude geophysical studies with satellite Injun 3," J. Geophys. Res. 69, 13-43, 1964.

33. Packer, D. M., "Altitudes of the night airglow radiations," Ann. Geophys., 17, 67-75, 1961.

34. Rapp, D. and D. D. Briglia, "Total cross sections for negative ion formation in gasses by electron impact," Lockheed Missile and Space Co., Tech. Rept. 6-74-64-40, 1964, a.

35. Rapp, D. T. E. Sharp and D. C. Briglia, "On the theoretical interpretation of resonance dissociative attachment cross sections," Lockheed Missile and Space Co., 6-74-64-45, 1964, b.

36. Reeves, R. R., G. Manella, and P. Harteck, "Rate of recombination of oxygen atoms," J. Chem. Phys. 32, 632-633, 1960.

37. Silverman, S. M. and E. N. Lassetre, "Collision cross sections for oxygen in the excitation energy range 10 to 80 V," J. Chem. Phys. 40, 2922-2932, 1964.

38. Tate, J. T. and P. T. Smith, "The efficiencies of ionization and ionization potential of various gases under electron impact," Phys. Res. 39, 270-273, 1932.

39. Wallace, L. "The OH nightglow emission," J. Atmos. Sci. 19, 1-16, 1962.

40. Watson, C. E., V. A. Dunlock Jr., R. S. Stolarski, and A. E. S. Green, "Electron impact cross sections for atmospheric species, 3, Molecular oxygen." J. Geophys. Res. 72, (5) 3961-3966, 1967.

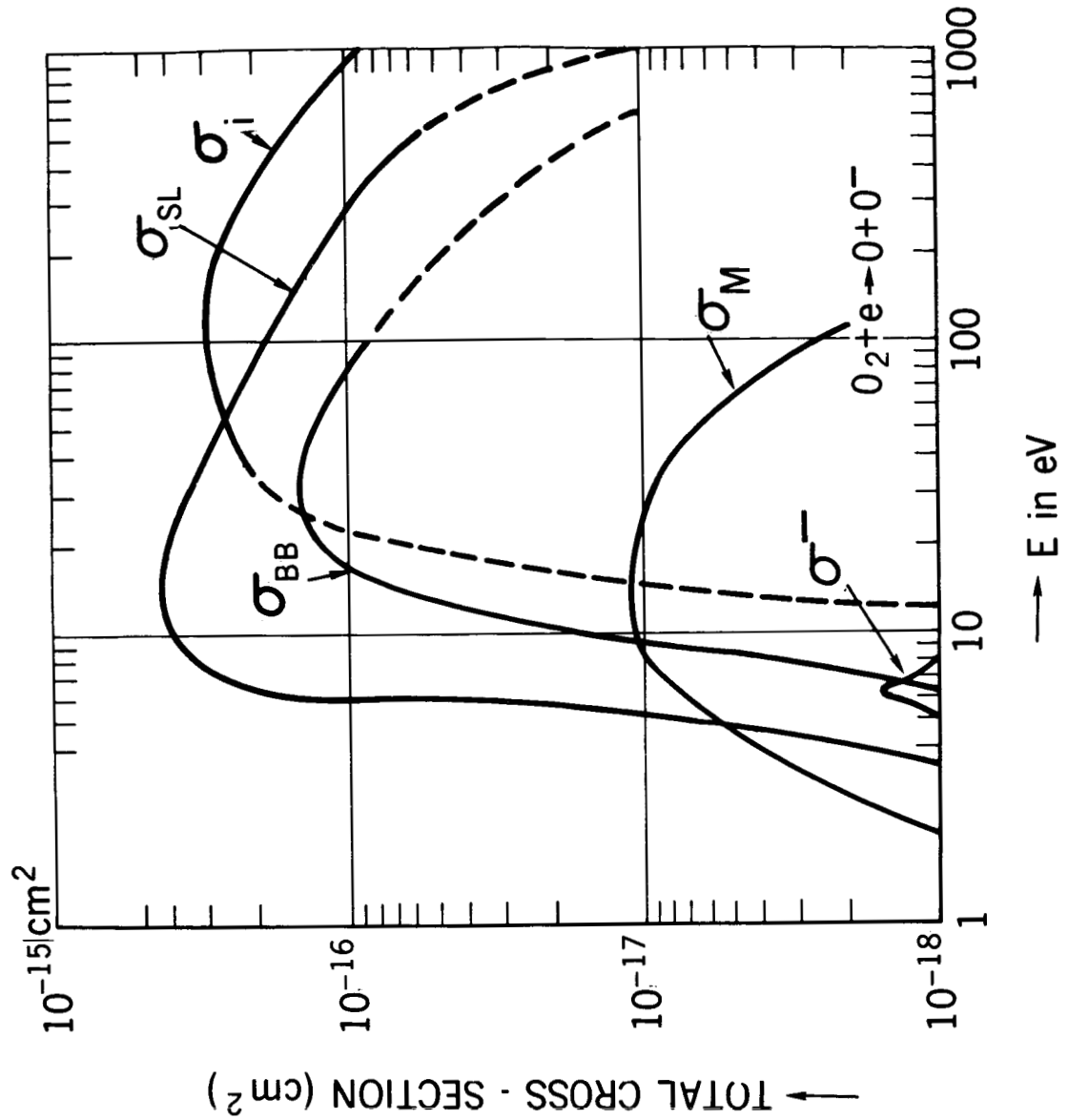

Figure 1. Total cross-sections of the O_2-dissociation by electron impacts. σ^-, σ_{SL} and σ_i are obtained by the laboratory experiments of Rapp et al (1964), Lassettre et al (1964) and Tates-Smith (1932), respectively. σ_{BB} and σ_M are the similar cross-section as σ_{SL}, calculated theoretically by Bauer and Bartky (1965), and the one derived by Maeda (1962, 1963), respectively.

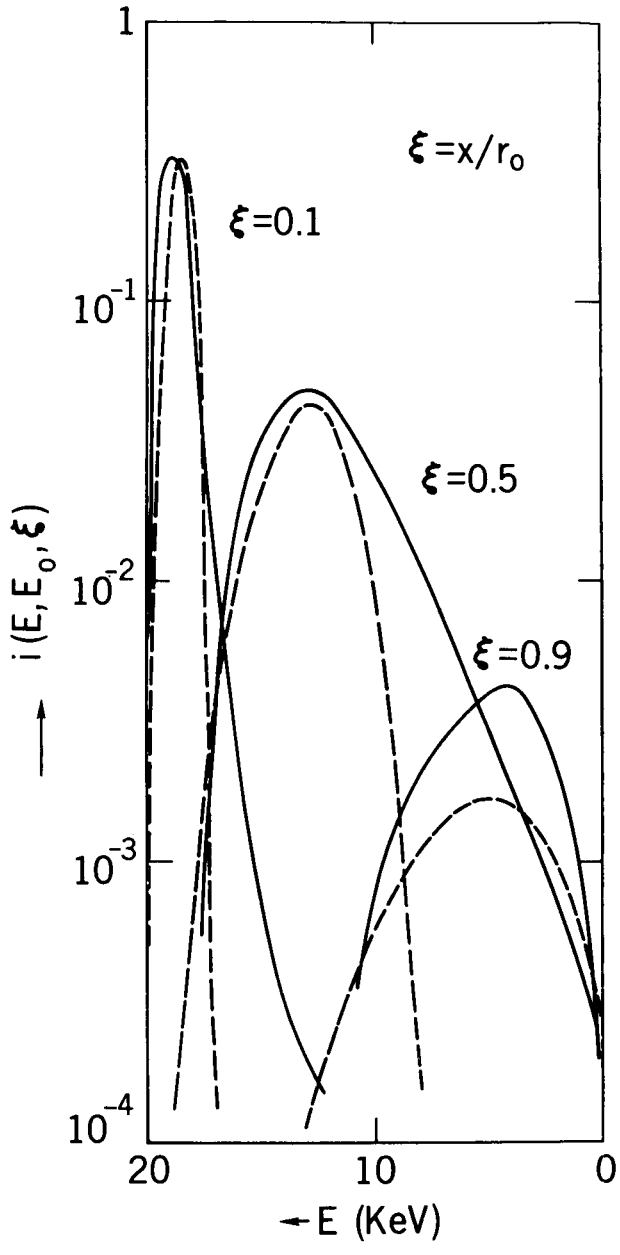

Figure 2. The changes of differential energy spectrum of the monoenergetically incident electrons, $i(E_0, E, \xi)$ with penetrating depth ξ. The full lines and dashed lines correspond to the direct results of Monte Carlo calculation and to those given by an empirical formula (Maeda and Aikin, 1967).

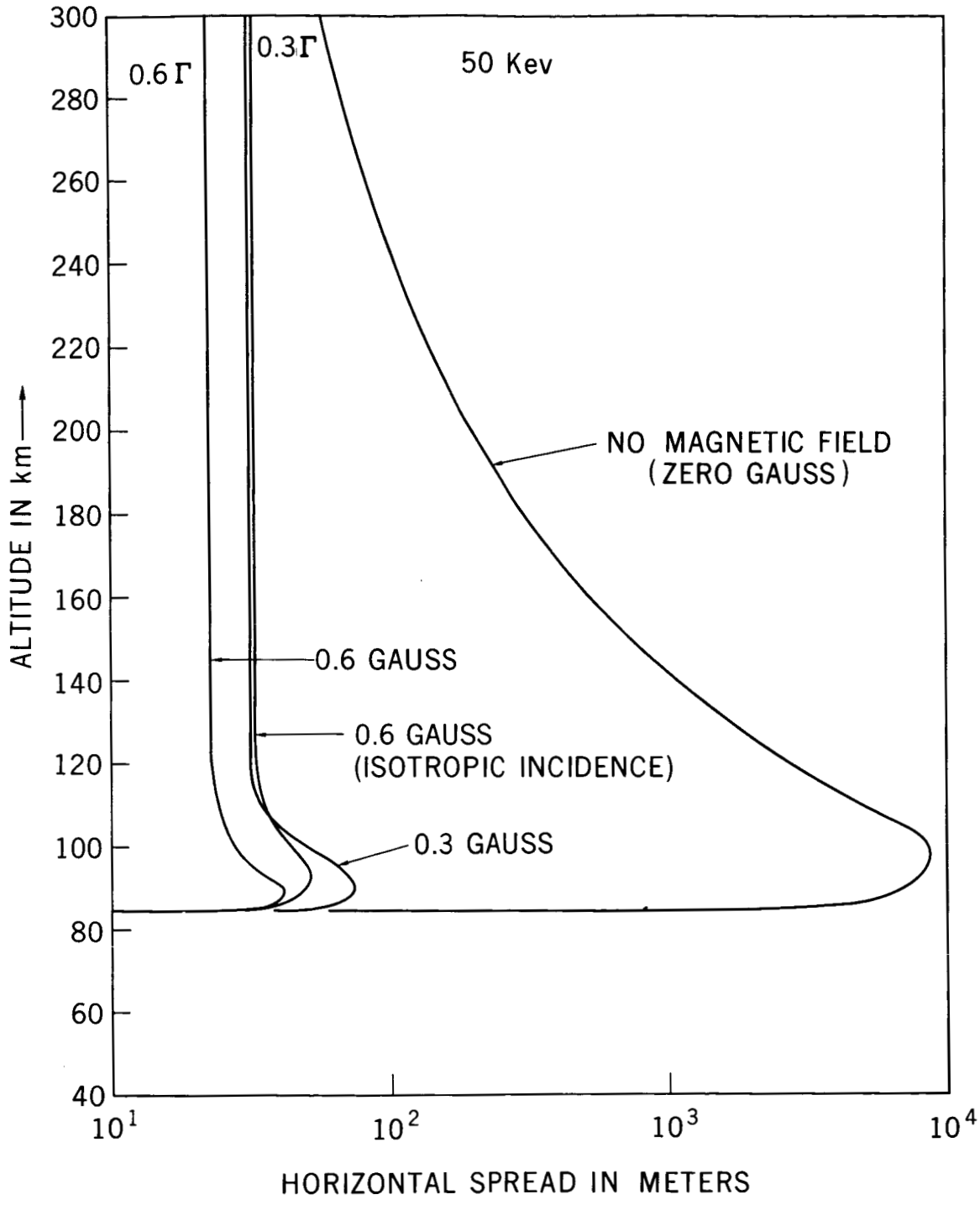

Figure 3. Horizontal spreads of vertically incident 50 kev electrons in the non-geomagnetic field atmosphere and in the atmosphere with vertical field 0.3 and 0.6 gauss, calculated by the Monte Carlo method.

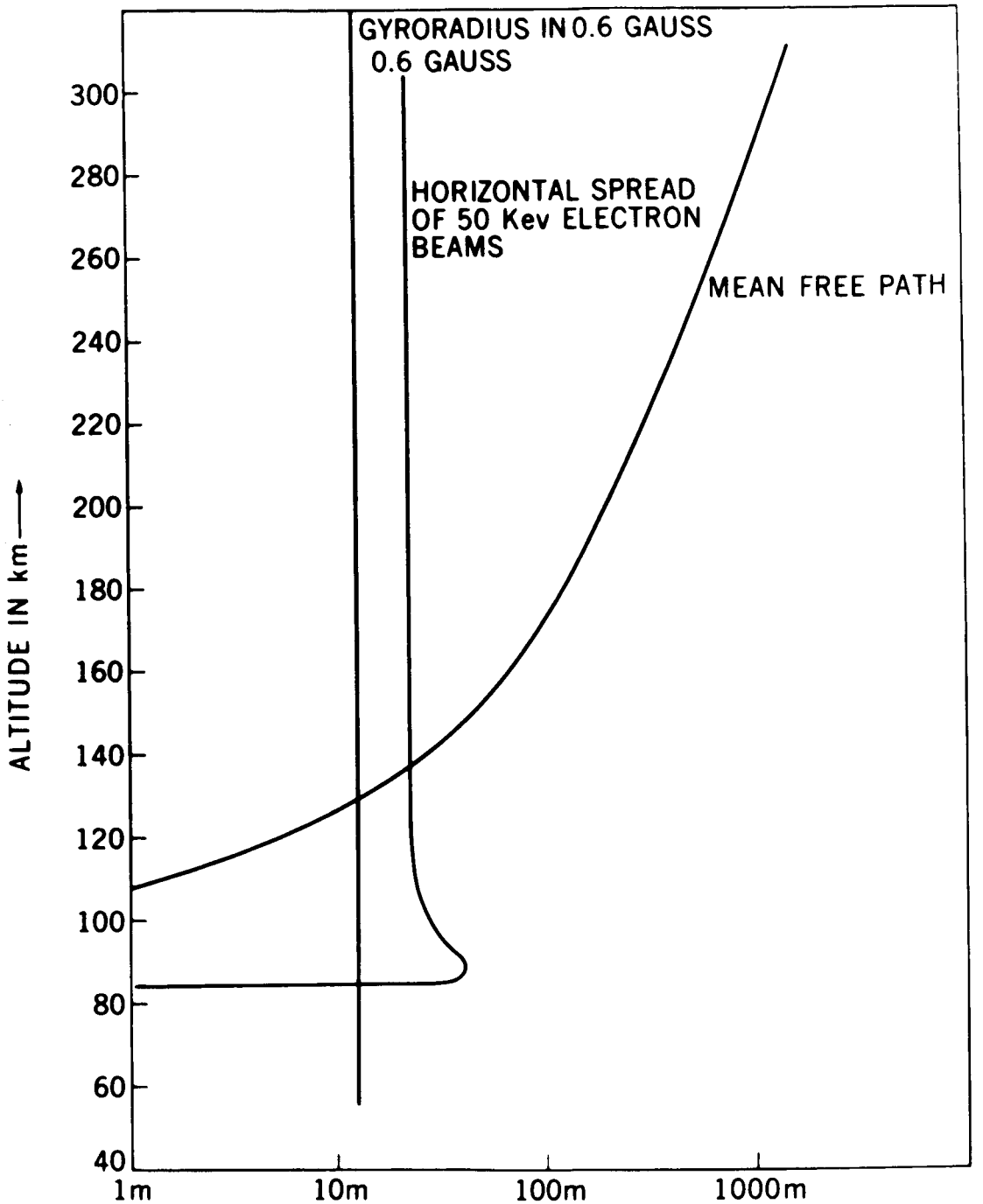

Figure 4. The gyroradius R_c (in meter) of 50 kev electrons in the vertical magnetic field of 0.6 gauss and the gas kinematic means free path of 50 kev electrons R_f (in meter) in the CIRA (1964) atmosphere, in comparison with the present result of the horizontal spread of 50 kev electrons in the CIRA (1964) atmosphere with 0.6 gauss field.

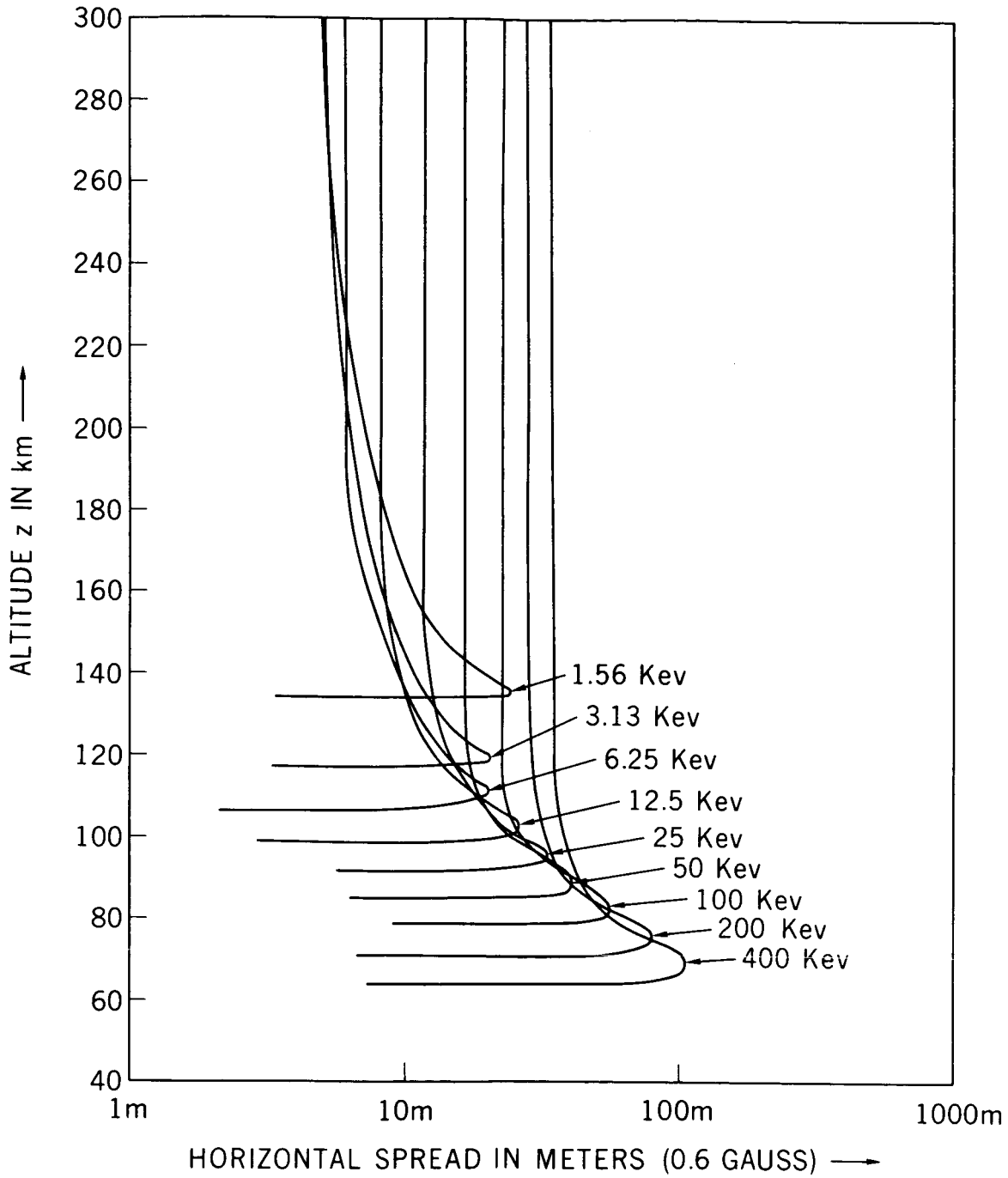

Figure 5. The horizontal spreads of electron beam in the CIRA (1964) atmosphere with vertical 0.6 gauss magnetic field for the incident energies, $E_0 = 400/n$ kev, where n = 1.2 . . . 8

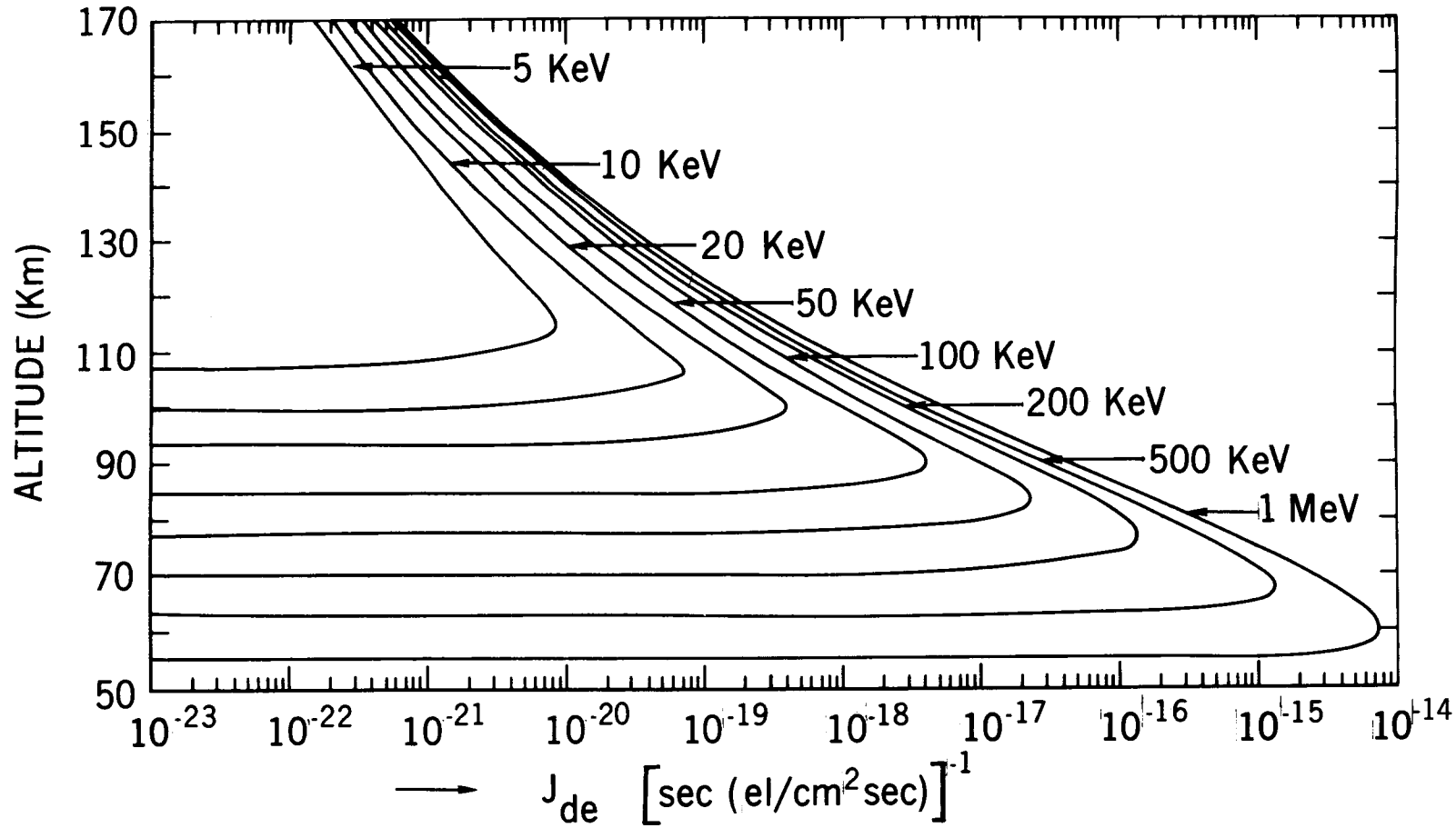

Figure 6. Rate coefficients of O_2-dissociation by unit flux of monoenergetic electrons $J_{de}(E_0, z)$ in sec^{-1} per (el/cm^2 sec) as the function of altitude z(in km).

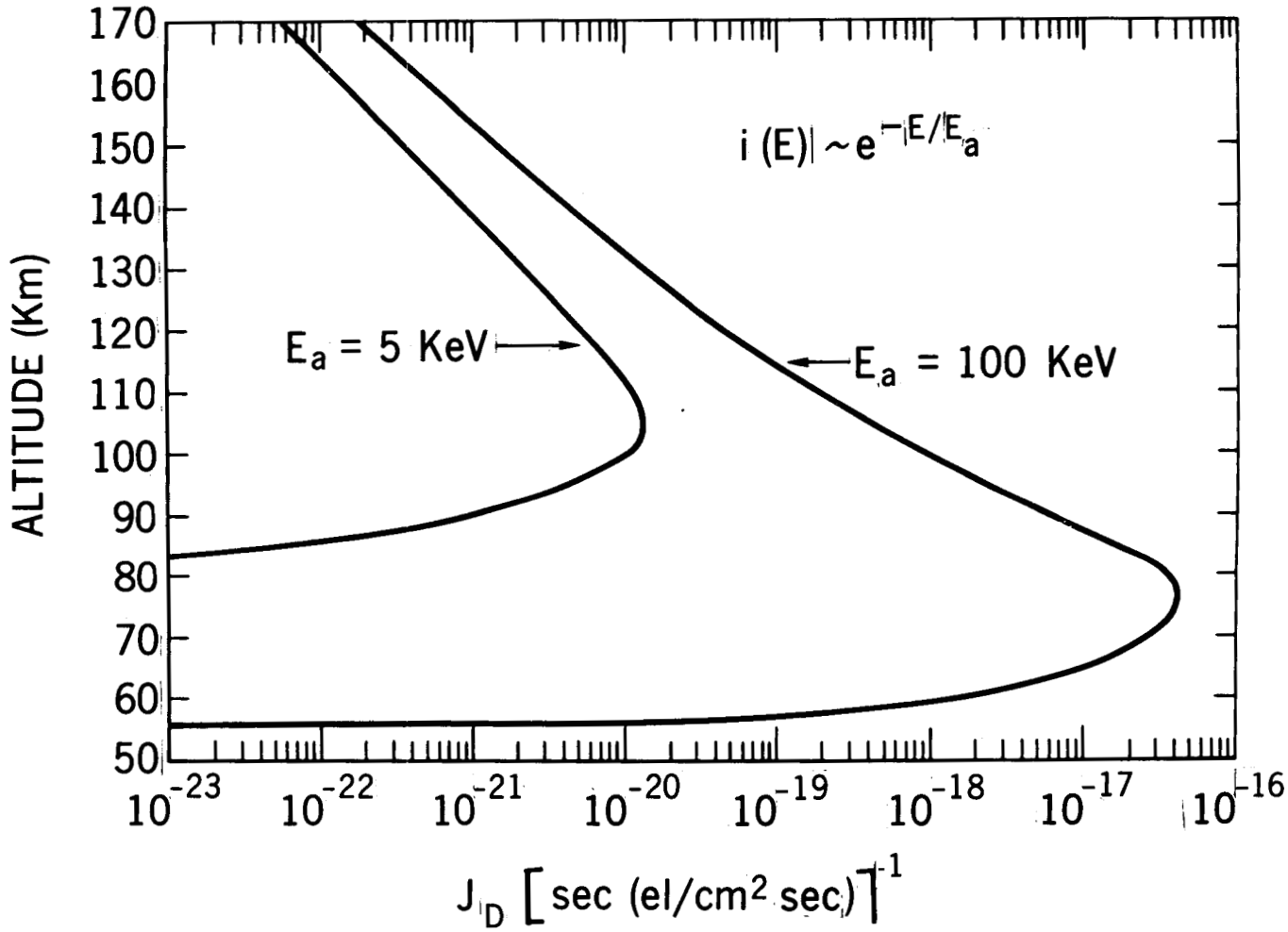

Figure 7. Rate coefficients of O_2 -dissociation by unit intensity of auroral electrons with differential energy spectrum

$$i(E_0) = i_0 \exp(-E_0/E_a)$$

Two curves correspond to E_a = 5 kev and E_a = 100 kev, respectively.

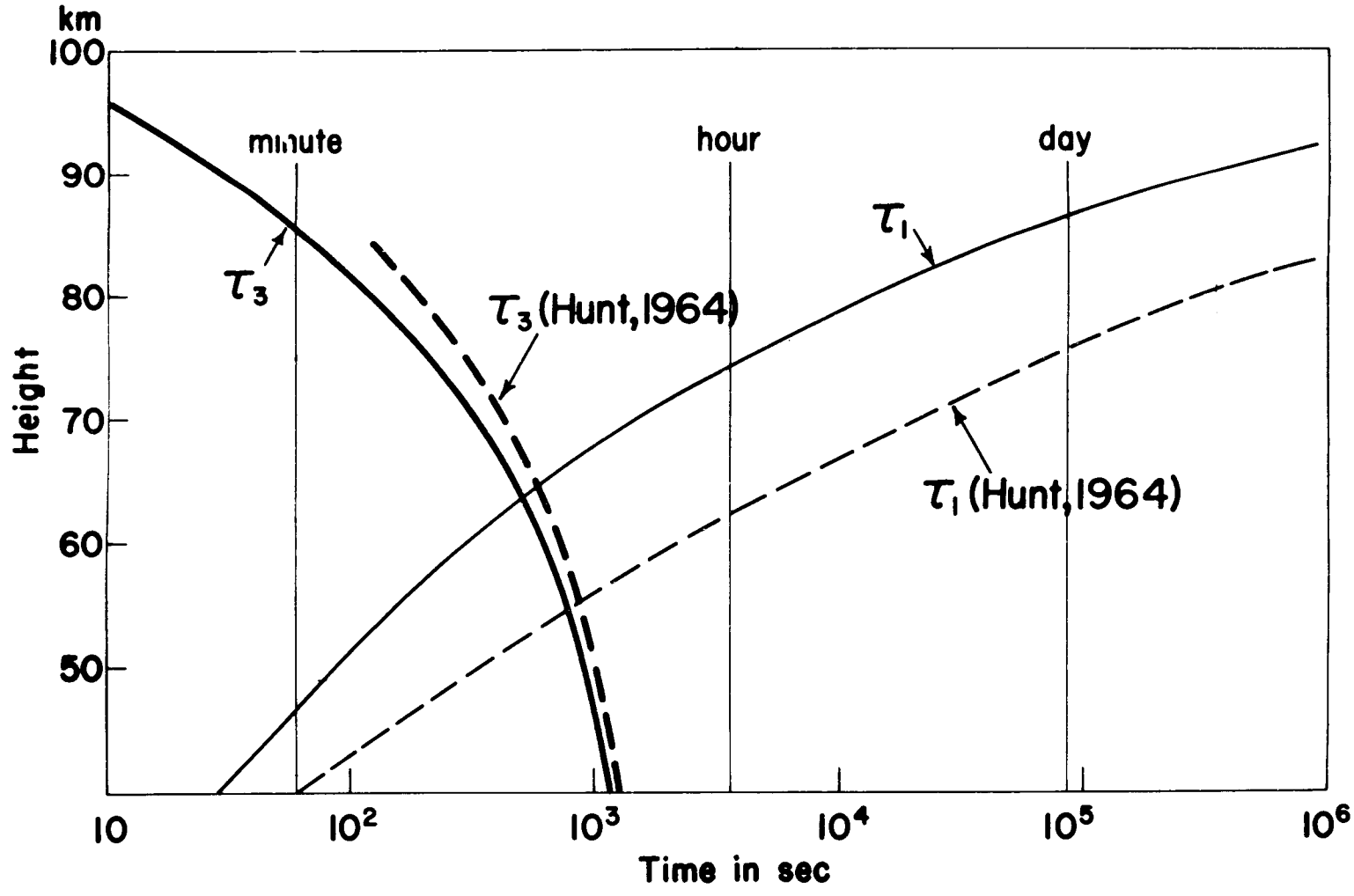

Figure 8. The altitude dependence of the relaxation time of atomics oxygen (τ_1) and of ozone (τ_3), in the pure-oxygen isothermal atmosphere. (MA-I, II)

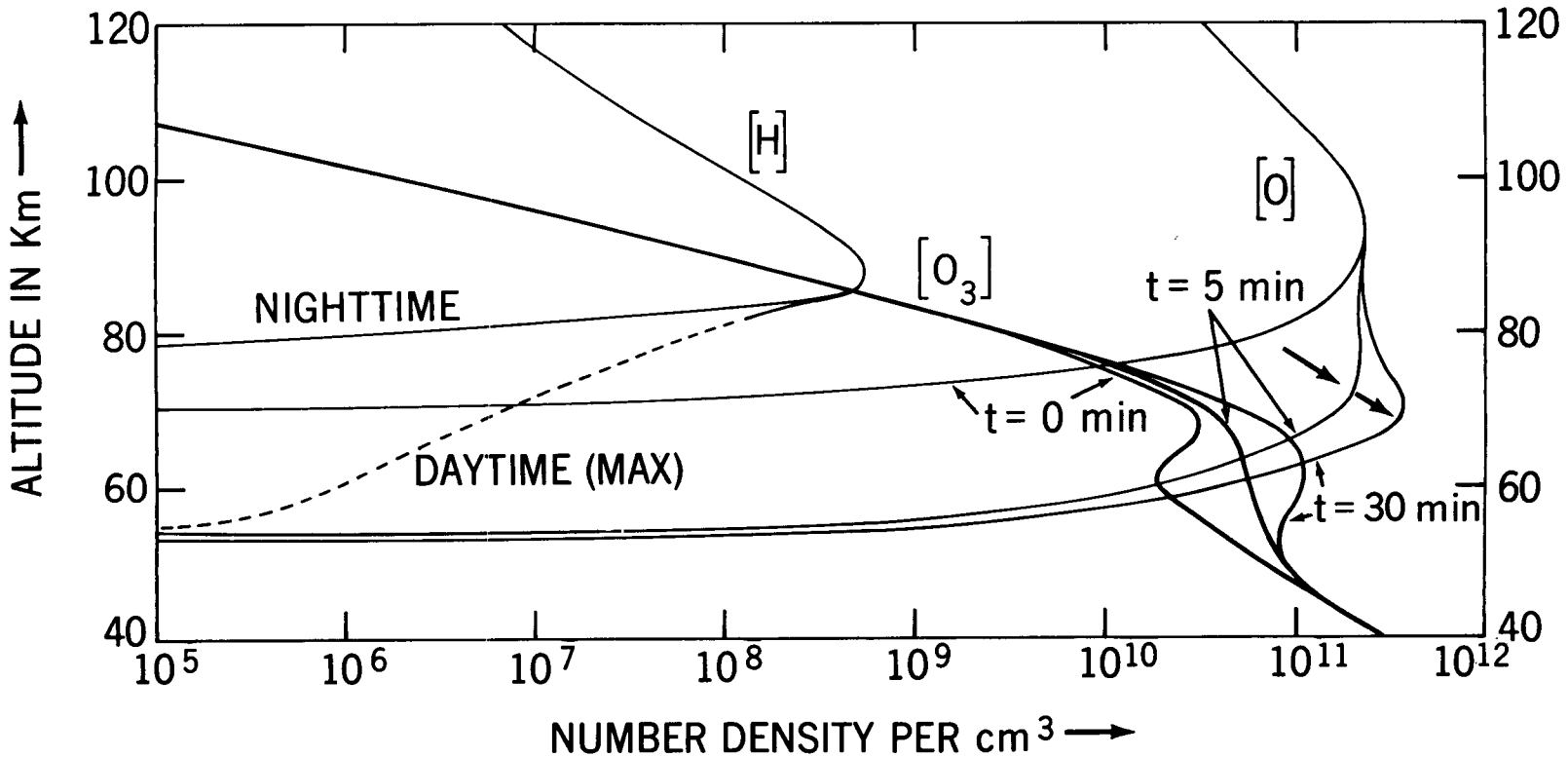

Figure 9. The altitude dependence of temporal variations of oxygen atom [O] , ozone [O_3] caused by the hard spectrum auroral electrons of 10^{10} cm^{-2} sec^{-1} flux in the atmosphere with constant atomic hydrogen distribution. The altitude distributions of atomic hydrogen [H] are shown by thin lines, and dashed line below around 85 km corresponds to the daytime maximum (Hunt, 1966).

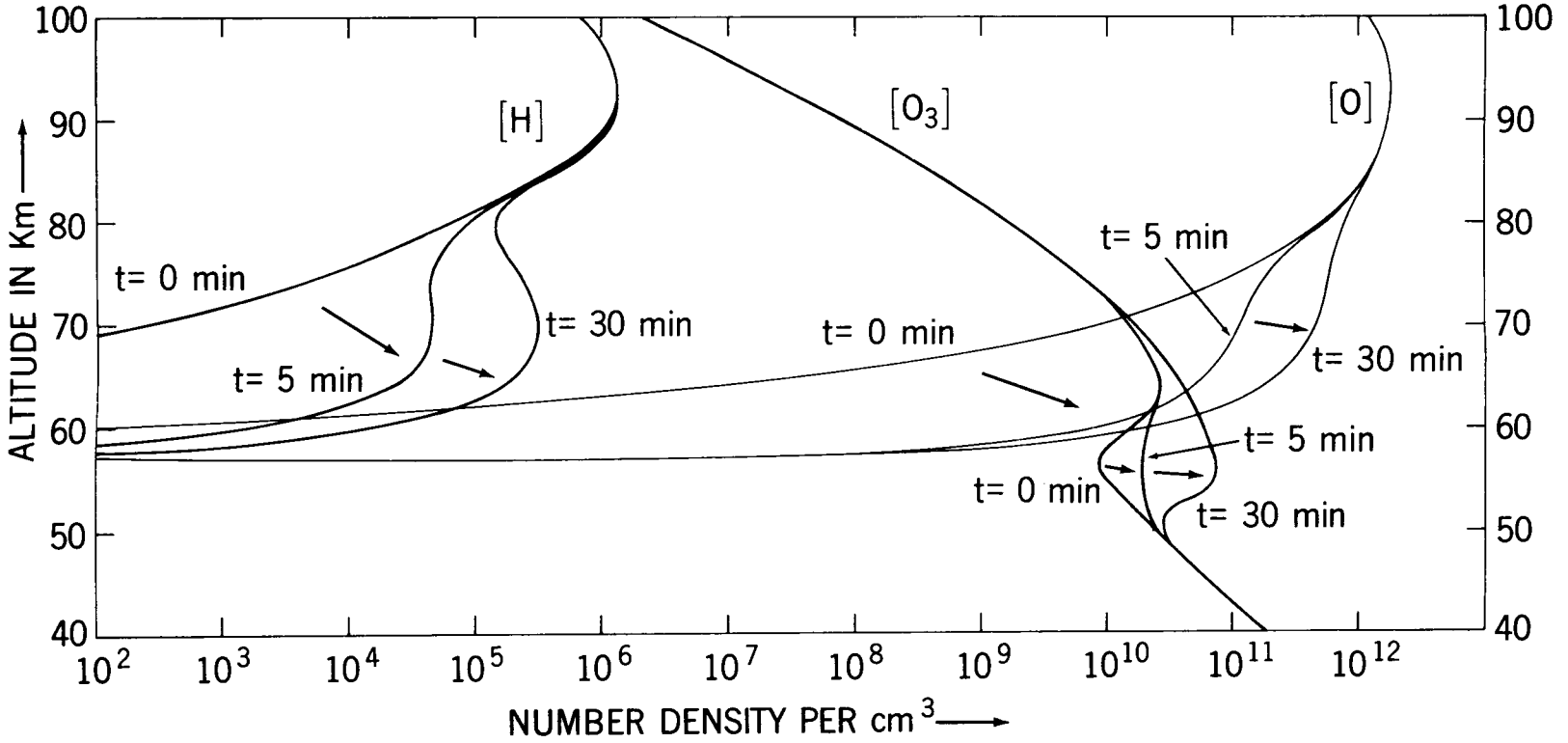

Figure 10. The altitude dependence of temporal variations of oxygen atom [O], ozone [O_3] and hydrogen atom [H] caused by the hard spectrum auroral electrons of 10^{10} cm^2 sec^{-1} flux.

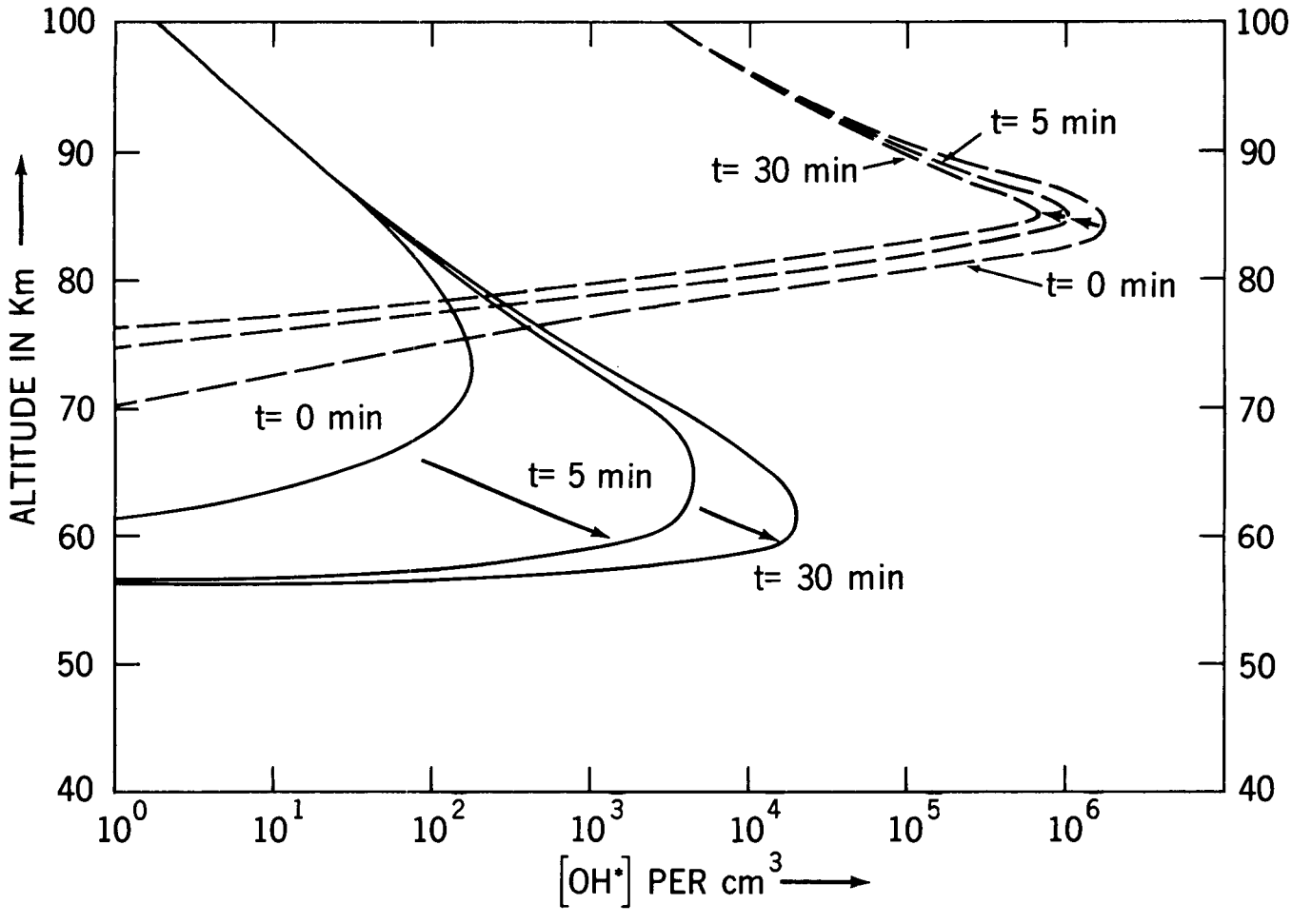

Figure 11. Temporal variation of hydroxyl concentration during the auroral events. The dashed lines correspond to the variations shown in Figure 9 (constant nighttime concentration of hydrogen atoms) and full lines correspond to the variations shown in Figure 10.

APPENDIX A

The mean horizontal radius R_0 is defined by

$$R_0(E_0, z) = \frac{\int_0^\infty R\, F(E_0, z, R,)\, dR}{\int_0^\infty F(E_0, z, R)\, dR} \qquad (A.1)$$

where $F(E_0, z, R)$ is the horizontal distribution function of energy dissipation per unit depth in a ring between radius R and R + dR, at the altitude z, corresponding to the initial (incident) energy of electrons E_0. In other words, if the energy deposition per unit depth at the altitude z is $D(E_0, z)$, then

$$D(E_0, z) = \int_0^\infty F(E_0, z, R)\, dR \qquad (\text{in eV/g cm}^{-2}) \qquad (A.2)$$

the energy dissipated per unit volume, $d(E_0, z)$ (in eV per cm^3) is

$$d(E_0, z) = \frac{F(E_0, z, R) \cdot \rho(z)}{2\pi R} \qquad (A.3)$$

where $\rho(z)$ is the atmospheric density at the altitude z ($g\ cm^{-3}$, z in km). The original Monte-Carlo calculations are made, using the atmospheric depth x (in g/cm^2). Transformations of all quantities as a function of altitude z are made with respect to the CIRA (1964)-atmosphere.

APPENDIX B

Time dependent chemical equations used in the calculations of the second order approximation are as follow;

$$\frac{d[O]}{dt} = A_1 - B_1 [O] - C_1 [O]^2 \qquad (B.1)$$

where

$$A_1 = 2J_2 [O_2] + J_3 [O_3] + J_4 [HO_2] + k_5 [H] [O_3] + k_{11} [H] [HO_2] + k_{15} [H] [OH] + k_{18} [OH] [O_3] + k_{19} [OH]^2 \qquad (B.1')$$

$$B_1 = k_2 [O_2] [M] + k_3 [O_3] + k_6 [OH] + k_8 [HO_2] + k_{10} [H] [M] \qquad (B.1'')$$

$$C_1 = k_1 [M] \qquad (B.1''')$$

$$\frac{d[O_2]}{dt} = A_2 - B_2 [O_2] \qquad (B.2)$$

where

$$A_2 = k_1 [O]^2 [M] + 2 \cdot k_3 [O] [O_3] + k_4 [H] [O_3] + k_6 [OH] [O] + k_8 [HO_2] [O] + k_{12} [H] [HO_2] + k_{20} [OH] [HO_2] \qquad (B.2')$$

$$B_2 = k_2 [O] [M] + k_7 [H] + k_9 [H] [M] \qquad (B.2'')$$

$$\frac{d[O_3]}{dt} = A_3 - B_3 [O_3] \qquad (B.3)$$

where

$$A_3 = k_2 [O] [O_2] [M] \qquad (B.3')$$

$$B_3 = J_3 + k_3 [O] + (k_4 + k_5) [H] + k_{18} [OH] \qquad (B.3'')$$

$$\frac{d[H]}{dt} = A_4 - B_4 [H] - C_4 [H]^2 \qquad (B.4)$$

where

$$A_4 = J_1 [H_2O] + k_6 [OH] [O] + k_{17} [H_2] [OH] \qquad (B.4')$$

$$B_4 = (k_4 + k_5) [O_3] + k_7 [O_2] + k_9 [O_2] [M] + k_{10} [O] [M] + (k_{11} + k_{12} + k_{13}) [HO_2] + k_{15} [OH] \qquad (B.4'')$$

$$C_4 = k_{14} [M] \qquad (B.4''')$$

$$\frac{d[H_2]}{dt} = A_5 - B_5 [H_2] \qquad (B.5)$$

where

$$A_5 = k_{12} [H] [HO_2] + k_{14} [H]^2 [M] + k_{15} [H] [OH] \qquad (B.5')$$

$$B_5 = k_{17} [OH] \qquad (B.5'')$$

$$\frac{d[OH]}{dt} = A_6 - B_6 [OH] - C_6 [OH]^2 \qquad (B.6)$$

where

$$A_6 = J_1 [H_2O] + J_4 [HO_2] + k_4 [H] [O_3] + k_8 [HO_2] [O] + k_{10} [H] [O] [M] + 2k_{13} [H] [HO_2] + k_{16} [H_2] [O] \quad (B.6')$$

$$B_6 = k_6 [O] + k_{15} [H] + k_{17} [H_2] + k_{18} [O_3] + k_{20} [HO_2] \quad (B.6'')$$

$$C_6 = k_{19} \quad (B.6''')$$

$$\frac{d[H_2O]}{dt} = A_7 - B_7 [H_2O] \quad (B.7)$$

where

$$A_7 = k_{11} [H] [HO_2] + k_{17} [H_2] [OH] + k_{19} [OH]^2 + k_{20} [OH] [HO_2] \quad (B.7')$$

$$B_7 = J_1 \quad (B.7'')$$

$$\frac{d[HO_2]}{dt} = A_8 - B_8 [HO_2] \quad (B.8)$$

where

$$A_8 = k_5 [H] [O_3] + k_9 [H] [O_2] [M] + k_{18} [OH] [O_3] \quad (B.8')$$

$$B_8 = k_8 [O] + (k_{11} + k_{12} + k_{13}) [H] + k_{20} [OH] \quad (B.8'')$$

The numerical values of rate coefficients are shown in Table 2.

In the actual calculations, two equations (B.2) and (B.8) are replaced by the following two conditions;

$$[O] + 2[O_2] + 3[O_3] + 2[HO_2] + [OH] + [H_2O] = \alpha[M] \qquad (B.9)$$

$$[H] + 2[H_2] + 2[H_2O] + [HO_2] + [OH] = \beta[M] \qquad (B.10)$$

where α and β are assumed to be 0.4 and 5.10^{-5}, indicating a relative abundance of oxygen and hydrogen at each level in the atmosphere, respectively (cf. Hesstvedt, 1964).